

INVESTIGATION OF THE $^{56}\text{Fe}(n, \gamma)^{57}\text{Fe}$ AND $^{58}\text{Fe}(n, \gamma)^{59}\text{Fe}$ REACTIONS

R. VENNINK and J. KOPECKY

*FOM-ECN Nuclear Structure Group, Netherlands Energy Research Foundation, Westerduinweg 3,
1755 ZG Petten, The Netherlands*

and

P. M. ENDT and P. W. M. GLAUDEMANS

Fysisch Laboratorium, Rijksuniversiteit Utrecht, Princetonplein 5, 3508 TA Utrecht, The Netherlands

Received 17 September 1979

(Revised 3 March 1980)

Abstract: The γ -radiation has been investigated produced by thermal neutron capture in a natural Fe sample and in a sample enriched in ^{58}Fe . Of the 253 γ -rays ascribed to the $^{56}\text{Fe}(n, \gamma)^{57}\text{Fe}$ reaction, 191 have been placed in the ^{57}Fe level scheme (of which 124 placements are new); of the 138 γ -rays observed in the $^{58}\text{Fe}(n, \gamma)^{59}\text{Fe}$ reaction 68 have been placed (with 55 new placements). Excitation energies (with 0.02–0.7 keV error) and branching ratios have been determined of 60 bound levels in ^{57}Fe and of 27 in ^{59}Fe . The Q -values of the $^{56, 58}\text{Fe}(n, \gamma)$ reactions amount to 7646.0 ± 0.2 and 6581.0 ± 0.2 keV, respectively. One can conclude that $J = \frac{3}{2}$ for the 2836 keV level in ^{57}Fe , and that $J^\pi = \frac{3}{2}^-$ for the 2570, 3072, 3104, 3160 and 3384 keV levels in ^{59}Fe .

A shell-model calculation has been performed with up to two holes in the $1f_{7/2}$ sub-shell and particles in the $2p_{3/2}$, $1f_{5/2}$ and $2p_{1/2}$ sub-shells. The energies of low-lying $^{57, 58, 59}\text{Fe}$ states are reproduced with a mean deviation of 0.17 MeV. The surface-delta interaction appears superior over the Kuo-Brown interaction in explaining the electromagnetic properties of the lowest six states of ^{57}Fe .

E

NUCLEAR REACTIONS $^{56, 58}\text{Fe}(n, \gamma)$, E = thermal; measured E_γ , I_γ ; deduced Q , $^{57, 59}\text{Fe}$ levels deduced E_x , γ -branching, J^π . Enriched and natural targets.

1. Introduction

Although a great deal of experimental work has been done on the level schemes of ^{57}Fe and ^{59}Fe , as reviewed in the compilations by Auble ¹⁾ and Kim ²⁾, respectively, thermal neutron capture has contributed relatively little.

Early $^{56}\text{Fe}(n, \gamma)^{57}\text{Fe}$ measurements with poor resolution have been reviewed by Bartholomew *et al.* ³⁾. Three later Ge(Li) measurements ^{4–6)} yielded more accurate results. The first paper ⁴⁾, however, only reports low-energy γ -rays ($E_\gamma < 2.9$ MeV), whereas in the second ⁵⁾ γ -ray energies and intensities are listed from a routine study of many elements with natural targets. The third investigation ⁶⁾ aimed at

establishing energy calibration standards; only strong high-energy transitions ($E_\gamma > 1.6$ MeV) are given.

On the $^{58}\text{Fe}(n, \gamma)^{59}\text{Fe}$ reaction at thermal energy only an exploratory experiment ⁷⁾ has been performed yielding 13 transitions with energy errors of 3–6 keV.

It was felt that it should be possible to obtain substantially more information on the thermal neutron capture γ -ray spectra for both ^{56}Fe and ^{58}Fe . In the present work singles Ge(Li) spectra have been measured with very good statistics and good resolution, covering the region from $E_\gamma = 200$ keV to above the neutron binding energy.

The energies of states in $^{57,58,59}\text{Fe}$ and the electromagnetic properties of low-lying states in ^{57}Fe have been compared to the results of a shell-model calculation taking into account up to two holes in the $1f_{7/2}$ sub-shell and particles in the $2p_{3/2}$, $1f_{5/2}$ and $2p_{1/2}$ sub-shells.

2. Experimental

The experiment has been performed at the High Flux Reactor in Petten. The target was placed in a beam of thermal neutrons with a flux of about $10^7 \text{ cm}^{-2} \cdot \text{s}^{-1}$. A natural iron sample was used for the $^{56}\text{Fe}(n, \gamma)$ reaction, while a sample, supplied by the Institute of Nuclear Research, Swierk, Poland, enriched to 62 % in ^{58}Fe was used in the $^{58}\text{Fe}(n, \gamma)$ measurement. Amounts of about 5 g were encapsulated in thin-walled cylindrical teflon tubes. A pure Cl and a mixed Cl-Fe sample together with radioactive sources were used for the energy and intensity calibration (see sect. 3).

The detection set-up consisted of a true axial Ge(Li) detector of 30 % efficiency with conventional electronics, coupled to a P9205 Philips on-line computer, for dumping the data on magnetic tape. The resolution of the detector was 2.2 keV for the 1.33 MeV ^{60}Co γ -ray.

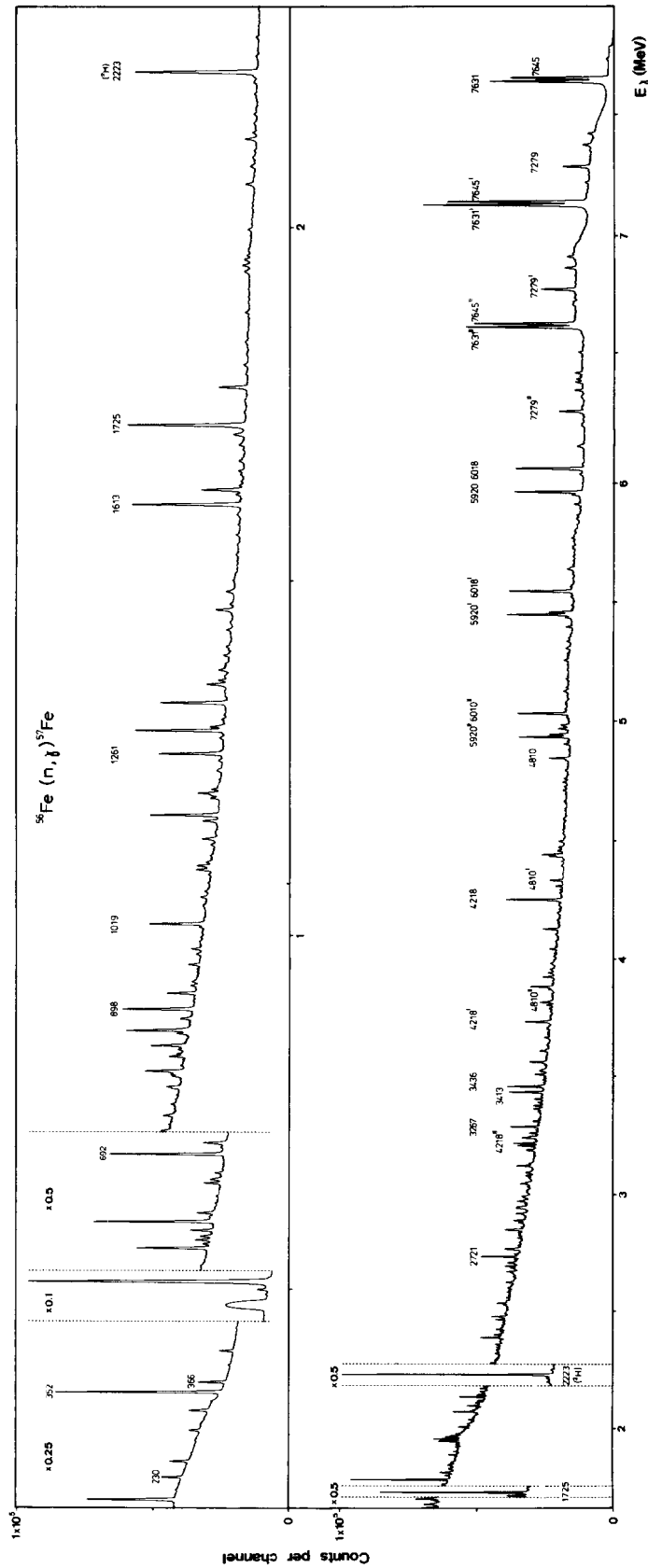
The measurements of the high-energy spectra (1.7–8.0) MeV took about 48 h each, whereas the measuring time for the low-energy spectra (0.1–2.3 MeV) was about 24 h. Fig. 1 shows the measured spectrum for the $^{56}\text{Fe}(n, \gamma)$ reaction with a natural Fe target. Only the γ -transitions in ^{57}Fe which are used for calibration of the ^{57}Fe and ^{59}Fe spectra are indicated in fig. 1.

3. Data analysis

3.1. CONTAMINANTS

In the measured spectra contaminant lines occur which have to be recognized as such.

The spectrum obtained with the natural Fe target shows, in addition to the lines



from the $^{56}\text{Fe}(n, \gamma)^{57}\text{Fe}$ reaction, the strongest lines resulting from capture in ^{54}Fe , ^{57}Fe and ^{58}Fe . By taking into account their relative abundances and thermal capture cross sections, one calculates that their contributions to the total spectrum amount to 5.0 %, 2.1 % and 0.14 %, respectively. The strongest lines due to ^{54}Fe and ^{57}Fe are well known from previous work ²⁹⁾, those due to ^{58}Fe from the present work.

Similarly the spectrum taken with the target enriched in ^{58}Fe had to be corrected for contributions from capture in ^{54}Fe , ^{56}Fe and ^{57}Fe , amounting to 2.5 %, 52.3 % and 3.4 %, respectively.

In addition, contaminant lines were observed due to ^1H , ^{14}N , ^{19}F , ^{27}Al , $^{70,72,73,74,76}\text{Ge}$ and ^{208}Pb , lines resulting from the $^{20}\text{F}(\beta^-\gamma)$ and $^{59}\text{Fe}(\beta^-\gamma)$ decays, and the 811 and 846 keV lines resulting from the (n, n') reaction on ^{58}Fe and ^{56}Fe , respectively, induced by epithermal neutrons.

Actually, no channel-by-channel subtraction has been performed for background or contaminant spectra from the main spectra, except for those narrow energy regions where contaminant lines close to main lines gave rise to complex peaks. The line shapes entering into such a quantitative deconvolution procedure are discussed below.

3.2. PEAK-FITTING PROCEDURE

The peak-fitting function consists of a gaussian distribution, provided with an asymmetric term to account for charge trapping and/or small-angle scattering. The whole expression contains four parameters, namely the peak position, full width at half maximum (FWHM), asymmetry parameter and peak area. Second-degree and linear adjustments as a function of E_γ were found to be satisfactory for FWHM and asymmetry parameter, respectively.

3.3. ENERGY AND INTENSITY CALIBRATION

The energy calibration curve for each spectrum was obtained by fitting a sixth-degree polynomial to the calibration energies. It is well-known ⁸⁾ that the energy differences between the full-energy peak and the single- and double-escape peaks can deviate from m_0c^2 and $2m_0c^2$, respectively. The magnitude of this deviation depends on geometrical properties of the detector. To account for this systematic effect these energy differences were used as free parameters. The values from the fitting procedure (amounting to 510.88 and 1021.64 keV, respectively) were used later for identification of single- and double-escape peaks, respectively.

Strong $^{35}\text{Cl}(n, \gamma)$ γ -rays from the mixed Cl-Fe sample, the ever present $\text{H}(n, \gamma)$ line, and γ -lines from radioactive sources were used for the energy calibration of strong ^{57}Fe transitions. These transitions were subsequently used in the ^{57}Fe and ^{59}Fe spectra as secondary calibration lines. The sources used were ^{54}Mn , ^{60}Co , ^{133}Ba and ^{137}Cs and the corresponding γ -energies were taken from ref. ⁹⁾. The Cl spectrum has recently been examined in detail by Spits *et al.* ¹⁰⁾ and independently

by Stelts *et al.* ⁶⁾. In the latter experiment only the high-energy part ($E_\gamma > 1.6$ MeV) of the $^{35}\text{Cl}(n, \gamma)$ spectrum was measured. In both investigations the neutron separation energy of ^{15}N , as determined from mass-spectroscopic work ¹¹⁾ was used for the energy calibration. The high-energy data ($E_\gamma > 4$ MeV) in the two experiments, however, show a systematic difference in the sense that the γ -ray energies of ref. ¹⁰⁾ are 0.2–0.4 keV lower than those of ref. ⁶⁾, which results in a difference of 42 ppm between the two measured Q -values for the $^{35}\text{Cl}(n, \gamma)$ reaction. If the Cl energies of ref. ¹⁰⁾ are used for calibration, the Q -value for the $^{56}\text{Fe}(n, \gamma)$ reaction from the present experiment is lower than the values reported previously from different (n, γ) precision experiments (see table 4). This may indicate that the energies reported in ref. ¹⁰⁾ are indeed systematically low. Application of the Cl data from ref. ⁶⁾ for the energy calibration leads to a Q -value consistent with the other data (see table 4). On this basis we decided to relate the absolute energy scale for the present Fe energies to that of ref. ⁶⁾, with a systematic uncertainty of 25 ppm, mainly due to the uncertainty reported in ref. ⁶⁾.

The detector efficiency calibration was performed for the low-energy part ($E_\gamma = 0.2$ – 2.0 MeV) with radioactive sources of known activity (^{54}Mn , ^{60}Co , ^{133}Ba , ^{137}Cs) and with the low-energy γ -rays recorded from a Cl target. For the high-energy part ($E_\gamma = 2.0$ – 8.6 MeV) only the high-energy γ -rays from a Cl target were used. The $^{35}\text{Cl}(n, \gamma)^{36}\text{Cl}$ intensities were taken from ref. ¹⁰⁾. At $E_\gamma \approx 2.0$ MeV the low- and high-energy parts were smoothly joined by requiring the equality of values and first derivatives.

3.4. PLACEMENT OF LINES; CALCULATION OF EXCITATION ENERGIES

The placement of lines is an iterative procedure which starts by tentatively placing the strongest lines between the levels known (often with large errors) from previous work. A least-squares calculation with the recoil-corrected transition energies as input values then yields more accurate excitation energies and the reaction Q -value. In each succeeding step the calculation is repeated with progressively more (weaker) lines added to the set of input values. A placement was rejected if it would have led to considerable imbalance between the intensity sums of incoming and outgoing transitions to and from a given level, respectively. It was also rejected if the J^π values of initial and final state (as known from previous and the present work) would have led to a transition character other than E1, M1 or E2. For none of the lines placed in this way does the energy deviate by more than three standard deviations from the corresponding difference in excitation energies. The same holds for the energy sums of all transitions forming a cascade between the capture state and the ground state.

The procedure described above does not lead to new levels, i.e. to levels not seen in previous work. One might try to search for new levels by fitting e.g. the energy sums of two unplaced transitions between two known levels. This has the drawback,

however, that one would not know which of the two transitions has to be placed highest in the level scheme. An analogous ambiguity would hold if one tries to fit energy differences of two unplaced transitions. Only γ - γ coincidence measurements could solve such difficulties, but they would be time consuming because all strong transitions have been placed ($I_\gamma > 0.7\%$ for ^{57}Fe , $I_\gamma > 1.0\%$ for ^{59}Fe ; see sect. 4).

4. Results and discussion

4.1. ^{57}Fe

Table 1 lists the energies, intensities and interpretation of the γ -rays ascribed to ^{57}Fe . Altogether 253 γ -rays have been observed of which 191 could be placed in the ^{57}Fe level scheme. The latter number represents an increase of 124 over the number of γ -rays placed previously ¹⁾. The lines which could not be placed are all quite weak; the strongest unplaced lines ($E_\gamma = 2753, 3103$ and 5731 keV) have intensities between 0.3% and 0.7% .

The energies of 20 strong low-energy lines ($E_\gamma < 2.9$ MeV) observed by Eissa and Honzátko ⁴⁾ agree with the present work within the rather large errors (0.3 – 2.0 keV) given by the former; for four additional lines deviations are observed of between one and three times the error. One of their lines ($E_\gamma = 705$ keV) proved to be a doublet. All their intensities are too high, for $E_\gamma > 600$ keV on the average by more than a factor of two.

The energies of 27 lines ($E_\gamma > 1.6$ MeV) listed by Stelts and Chrien ⁶⁾ are in excellent agreement with the present work; there are no deviations exceeding twice the combined error. The good agreement is to be expected because their $^{35}\text{Cl}(n, \gamma)$ energies formed the basis for the present energy calibration (see subsect. 3.2). Their intensities also agree very well, except for the $E_\gamma = 2.0$ – 3.5 MeV region where they are on the average about 30% higher.

Table 2 gives the excitation energies, the intensity balance and the primary γ -ray branching for the 61 bound states excited in the (n, γ) reaction. This number compares with 13 states observed certainly (and an additional 19 states observed possibly) from previous (n, γ) work ¹⁾. The accuracy in the energies of the levels both seen at present and previously in (n, γ) has been increased on the average by almost an order of magnitude. Three of the levels from previous work (at $E_x = 1019, 2147$ and 3278 keV) indicated as “possible” have been shown not to exist. The previous (d, p) work ¹⁴⁾ (yielding the entries in column two without assigned errors) apparently has provided surprisingly accurate energies; the differences with the energies from the present work are all below 6 keV. The existence has been proven of 12 levels listed as tentative in the $A = 57$ compilation ¹⁾ (the corresponding energies are bracketed in column two).

The intensity balance for strongly excited states is satisfactory, if a 10% systematic γ -ray intensity error is taken into account. Amongst the medium strongly excited

TABLE I
Gamma-rays from the $^{56}\text{Fe}(n, \gamma)^{57}\text{Fe}$ reaction

E_γ ^{a)}	I_γ ^{b)}	$E_{x_i} \rightarrow E_{x_f}$ ^{c)} (keV)	E_γ ^{a)}	I_γ ^{b)}	$E_{x_i} \rightarrow E_{x_f}$ ^{c)} (keV)
122.08(2)	— ^{d)}	136 \rightarrow 14	1197.27(6)	0.36(2)	5179 \rightarrow 3982
136.52(2)	— ^{d)}	136 \rightarrow 0	1215.38(4)	0.10(2)	4137 \rightarrow 2922
211.87(9)	0.08(1)	3183 \rightarrow 2971	1218.55(4)	0.07(1)	
230.29(2)	0.87(5)	367 \rightarrow 136	1250.99(9)	0.12(2)	1265 \rightarrow 14
251.1(3)	0.04(1)	1977 \rightarrow 1725	1255.5(8)	0.02(1)	4379 \rightarrow 3123
335.9(3)	0.04(1)	4379 \rightarrow 4043	1260.60(3)	2.50(8)	1627 \rightarrow 367
339.54(18)	0.08(1)	706 \rightarrow 367	1263.3(3)	0.10(1)	3240 \rightarrow 1977
352.36(1)	9.5(5)	367 \rightarrow 14	1282.3(6)	0.09(4)	4137 \rightarrow 2855
366.75(1)	1.68(8)	367 \rightarrow 0	1284.0(5)	0.10(5)	3982 \rightarrow 2697
460.1(4)	0.03(1)	1725 \rightarrow 1265	1300.9(4)	0.09(2)	4137 \rightarrow 2836
564.19(6)	0.22(1)	3323 \rightarrow 2758	1305.5(3)	0.07(2)	4210 \rightarrow 2904
569.92(4)	0.52(3)	706 \rightarrow 136	1345.2(5)	0.06(1)	3323 \rightarrow 1977
575.09(19)	0.19(10)	4137 \rightarrow 3561	1351.8(10)	0.05(2)	4460 \rightarrow 3099
598.63(14)	0.22(2)		1355.6(4)	0.13(3)	4692 \rightarrow 3337
601.3(2)	0.14(2)	4210 \rightarrow 3609	1358.71(4)	0.90(4)	1725 \rightarrow 367
603.54(19)	0.16(2)	2821 \rightarrow 2218	1369.1(2)	0.13(2)	4692 \rightarrow 3323
657.56(9)	0.25(3)	2988 \rightarrow 2330	1371.6(4)	0.06(2)	
692.03(2)	4.75(19)	706 \rightarrow 14	1381.7(2)	0.13(1)	3982 \rightarrow 2600
703.4(4)	0.05(2)	2330 \rightarrow 1627	1412.01(12)	0.17(1)	
706.4(2)	0.27(10)	706 \rightarrow 0	1430.2(4)	0.04(1)	
723(2)	0.01(1)	2836 \rightarrow 2113	1435.58(8)	0.22(1)	
735.1(3)	0.04(1)	3240 \rightarrow 2505	1447.0(3)	0.08(2)	3561 \rightarrow 2113
747.31(7)	0.12(2)		1457.4(5)	0.04(1)	3183 \rightarrow 1725
749.4(4)	0.04(1)		1460.9(3)	0.08(1)	3792 \rightarrow 2330
803.09(8)	0.21(1)	3561 \rightarrow 2758	1487.2(9)	0.03(1)	4692 \rightarrow 3206
818.6(3)	0.04(1)		1492.4(4)	0.06(1)	2758 \rightarrow 1265
834.91(8)	0.21(1)	4137 \rightarrow 3302	1506.0(2)	0.08(1)	
837.9(3)	0.07(1)	2564 \rightarrow 1725	1584.6(3)	0.07(1)	3792 \rightarrow 2207
849.5(5)	0.04(1)	2113 \rightarrow 1265	1612.78(2)	5.38(16)	1627 \rightarrow 14
870.75(17)	0.17(1)	1007 \rightarrow 136	1627.05(7)	0.21(1)	1627 \rightarrow 0
884.78(10)	0.28(2)	3340 \rightarrow 2455	1646.0(3)	0.07(1)	3371 \rightarrow 1725
898.28(2)	1.90(8)	1265 \rightarrow 367	1655.51(11)	0.15(2)	3862 \rightarrow 2207
920.85(2)	0.76(4)	1627 \rightarrow 706	1672.1(8)	0.04(2)	
942.0(14)	0.02(1)	2207 \rightarrow 1265	1674.62(12)	0.08(2)	3302 \rightarrow 1627
977.1(7)	0.05(3)	3183 \rightarrow 2207	1691.0(10)	0.07(1)	
988.2(5)	0.03(1)	3206 \rightarrow 2218	1697.34(12)	0.27(2)	
991.8(5)	0.04(1)	1007 \rightarrow 14	1700.8(3)	0.11(2)	4460 \rightarrow 2758
1006.9(5)	0.03(1)	4379 \rightarrow 3371	1705.0(8)	0.03(1)	4210 \rightarrow 2505
1019.02(2)	1.74(5)	1725 \rightarrow 706	1710.2(3)	0.25(5)	1725 \rightarrow 14
1022.0(3)	0.05(1)	3240 \rightarrow 2218	1717.2(3)	0.07(1)	
1026.4(3)	0.05(1)	4210 \rightarrow 3183	1722.40(12)	0.33(3)	2988 \rightarrow 1265
1041.1(5)	0.03(1)	3371 \rightarrow 2330	1725.29(3)	6.3(3)	1725 \rightarrow 0
1043.9(4)	0.07(1)		1760.1(2)	0.12(1)	
1077.3(3)	0.04(1)	4137 \rightarrow 3059	1802.3(6)	0.04(1)	
1110.9(3)	0.05(1)	4210 \rightarrow 3099	1810.51(16)	0.25(2)	3536 \rightarrow 1725
1115.64(15)	0.09(1)	3323 \rightarrow 2207	1812.9(5)	0.07(2)	2821 \rightarrow 1007
1119.8(6)	0.02(1)	4460 \rightarrow 3340	1825.9(3)	0.09(2)	3183 \rightarrow 1357
1159.5(13)	0.02(1)	3982 \rightarrow 2821	1828.9(10)	0.03(2)	2836 \rightarrow 1007
1186.0(5)	0.04(1)		1836.4(4)	0.06(1)	4692 \rightarrow 2855

TABLE I (continued)

$E_\gamma^a)$	$I_\gamma^b)$	$E_{xi} \rightarrow E_{xf}^c)$ (keV)	$E_\gamma^a)$	$I_\gamma^b)$	$E_{xi} \rightarrow E_{xf}^c)$ (keV)
1841.9(4)	0.09(3)		2537.1(5)	0.08(2)	2904 \rightarrow 367
1851.3(4)	0.06(1)	2218 \rightarrow 367	2562.4(5)	0.04(1)	2564 \rightarrow 0
1855.9(4)	0.06(1)	4692 \rightarrow 2836	2574.3(3)	0.11(2)	5140 \rightarrow 2564
1899.5(5)	0.06(2)	5140 \rightarrow 3240	2582.0(3)	0.09(2)	4210 \rightarrow 1627
1927.6(5)	0.04(2)		2598.1(11)	0.03(1)	2600 \rightarrow 0
1931.8(7)	0.06(2)	4137 \rightarrow 2207	2603.1(5)	0.07(2)	2971 \rightarrow 367
1943.1(5)	0.29(12)		2618.9(9)	0.05(2)	2988 \rightarrow 367
1965.3(2)	0.29(3)	3323 \rightarrow 1357	2654.3(4)	0.05(2)	4379 \rightarrow 1725
1973.4(4)	0.15(2)	4572 \rightarrow 2600	2682.5(3)	0.43(2)	2697 \rightarrow 14
1976.4(11)	0.04(2)	1977 \rightarrow 0	2691.6(5)	0.07(2)	3059 \rightarrow 367
1982.1(4)	0.08(2)	3609 \rightarrow 1627	2696.6(3)	0.30(4)	2697 \rightarrow 0
1987.0(7)	0.04(1)		2704.6(9)	0.05(2)	
1991.0(10)	0.03(1)	2697 \rightarrow 706	2721.17(6)	1.37(4)	3428 \rightarrow 706
2033.2(2)	0.05(2)	4598 \rightarrow 2564	2734.2(3)	0.15(2)	4460 \rightarrow 1725
2039.7(4)	0.05(1)		2753.0(2)	0.42(3)	
2045.7(4)	0.07(1)		2755.9(2)	0.57(10)	3123 \rightarrow 367
2066.17(11)	0.49(3)	3792 \rightarrow 1725	2815.0(6)	0.09(2)	3183 \rightarrow 367
2068.9(5)	0.11(3)		2821.5(2)	0.10(2)	2836 \rightarrow 14
2081.2(3)	0.10(2)	2218 \rightarrow 136	2832.46(17)	0.53(4)	4460 \rightarrow 1627
2091.85(15)	0.38(3)	3099 \rightarrow 1007	2835.43(17)	0.25(3)	2836 \rightarrow 0
2097(2)	0.05(3)	4210 \rightarrow 2113	2873.7(3)	0.37(2)	3240 \rightarrow 367
2101.3(14)	0.08(4)		2935.8(8)	0.05(2)	3302 \rightarrow 367
2104.5(5)	0.14(3)	3302 \rightarrow 1197	2943.4(5)	0.08(2)	4210 \rightarrow 1265
2113.4(3)	0.15(2)	2113 \rightarrow 0	2950.2(9)	0.07(2)	
2129.48(7)	0.67(3)	2836 \rightarrow 706	2954.04(17)	0.36(3)	C \rightarrow 4692
2138.63(17)	0.17(2)	2505 \rightarrow 367	2970.3(3)	0.18(2)	3337 \rightarrow 367
2151.5(2)	0.17(2)		3014.7(3)	0.12(2)	5222 \rightarrow 2207
2164.69(17)	0.20(2)	3792 \rightarrow 1627	3027.55(13)	0.11(1)	5140 \rightarrow 2113
2186.6(4)	0.04(1)	4692 \rightarrow 2505	3047.9(7)	0.04(1)	C \rightarrow 4598
2192.8(4)	0.25(4)	2207 \rightarrow 14	3060.90(15)	0.15(2)	3428 \rightarrow 367
2198.2(5)	0.17(4)	2904 \rightarrow 706	3075.1(5)	0.11(5)	C \rightarrow 4572
2202.7(8)	0.13(4)	2218 \rightarrow 14	3103.1(4)	0.67(7)	
2206.8(6)	0.21(5)	2207 \rightarrow 0	3166.9(11)	0.16(13)	3183 \rightarrow 14
2216.2(5)	0.12(4)	2922 \rightarrow 706	3186.0(2)	0.68(3)	C \rightarrow 4460
2246.0(5)	0.11(2)		3225.3(4)	0.30(5)	3240 \rightarrow 14
2348.9(9)	0.06(3)	4460 \rightarrow 2113	3239.3(2)	0.35(3)	3240 \rightarrow 0
2351.7(5)	0.11(3)		3267.05(12)	1.29(5)	C \rightarrow 4379
2385.3(4)	0.09(2)	5222 \rightarrow 2836	3291.1(2)	0.30(5)	3428 \rightarrow 136
2391.8(2)	0.22(2)	2758 \rightarrow 367	3356.3(2)	0.34(2)	3371 \rightarrow 14
2407.4(4)	0.10(2)	C \rightarrow 5238	3412.90(9)	1.61(8)	3428 \rightarrow 14
2415.1(3)	0.16(2)	4043 \rightarrow 1627	3436.4(3)	1.63(11)	C \rightarrow 4210
2424.3(9)	0.06(2)	C \rightarrow 5222	3504.5(8)	0.18(5)	C \rightarrow 4144
2462.1(7)	0.07(2)	2600 \rightarrow 136	3508.6(5)	0.05(3)	C \rightarrow 4137
2466.0(9)	0.08(2)	C \rightarrow 5179	3610.2(8)	0.05(2)	5238 \rightarrow 1627
2480.2(6)	0.06(2)	5179 \rightarrow 2697	3641.33(15)	0.20(6)	
2486.0(6)	0.08(2)	4692 \rightarrow 2207	3649(2)	0.03(2)	
2490.8(13)	0.03(1)	2505 \rightarrow 14	3663.0(2)	0.13(1)	C \rightarrow 3982
2507.2(7)	0.04(1)	C \rightarrow 5140	3689.4(7)	0.06(2)	
2517.0(5)	0.10(3)	4144 \rightarrow 1627	3710.9(5)	0.07(2)	
2526.2(3)	0.29(6)	3792 \rightarrow 1265	3723.6(7)	0.18(3)	
2534.0(6)	0.06(2)		3776.6(2)	0.08(3)	3792 \rightarrow 14

TABLE 1 (continued)

E_γ ^{a)}	I_γ ^{b)}	$E_{xi} \rightarrow E_{xf}$ ^{c)} (keV)	E_γ ^{a)}	I_γ ^{b)}	$E_{xi} \rightarrow E_{xf}$ ^{c)} (keV)
3842.4(3)	0.29(2)	4210 \rightarrow 367	4856.6(13)	0.10(4)	5222 \rightarrow 367
3854.0(2)	0.19(2)	C \rightarrow 3792	4914(2)	0.15(9)	
3921.5(7)	1.34(8)	3936 \rightarrow 14	4948.3(3)	0.85(8)	C \rightarrow 2697
3955.3(8)	0.11(3)		5042.1(8)	0.18(5)	5179 \rightarrow 136
3981.7(4)	0.10(2)	3982 \rightarrow 0	5047.4(10)	0.17(5)	C \rightarrow 2600
3991(2)	0.05(2)		5179.7(8)	0.05(3)	
4073.3(3)	0.21(2)	4210 \rightarrow 136	5318(2)	0.09(4)	C \rightarrow 2330
4194.8(4)	0.13(3)	4210 \rightarrow 14	5325.8(10)	0.18(3)	
4210.2(10)	0.07(2)	4210 \rightarrow 0	5730.64(15)	0.46(5)	
4217.98(11)	3.77(19)	C \rightarrow 3428	5784.9(7)	0.19(3)	
4274.5(2)	0.25(5)	C \rightarrow 3371	5901.4(12)	0.19(6)	
4323.8(4)	0.12(3)	C \rightarrow 3323	5920.35(7)	9.6(7)	C \rightarrow 1725
4378.3(4)	0.16(2)	4379 \rightarrow 0	5992(2)	0.22(16)	
4405.74(8)	1.64(8)	C \rightarrow 3240	6018.42(7)	9.9(8)	C \rightarrow 1627
4418.2(3)	0.13(4) ^{e)}		6102.1(10)	0.05(2)	
4462.5(4)	0.52(5)	C \rightarrow 3183	6129.3(4)	0.12(3)	
4555.5(3)	0.09(2)	4692 \rightarrow 136	6219.4(13)	0.08(3)	
4597.4(5)	0.15(3)		6276.4(4)	0.12(4) ^{e)}	
4659.3(6)	0.09(3)	C \rightarrow 2988	6380.47(15)	1.11(12)	C \rightarrow 1265
4675.1(2)	0.40(4)	C \rightarrow 2971	6548.5(8)	0.16(4) ^{e)}	
4687(2)	0.11(8)		6717.4(2)	0.45(4) ^{e)}	
4724.0(3)	0.28(3)	C \rightarrow 2922	6742(2)	0.12(6)	
4809.83(14)	1.85(11)	C \rightarrow 2836	7199(2)	0.10(4)	
4825.6(13)	0.07(3)	C \rightarrow 2821	7278.82(9)	6.0(6)	C \rightarrow 367
4840(2)	0.07(3)		7631.18(10)	29(4)	C \rightarrow 14
4845.5(5)	0.10(3)		7645.58(10)	25(3)	C \rightarrow 0

^{a)} Errors are statistical; to account for the uncertainty in the energy calibration, a systematic error of 25 ppm should be added quadratically.

^{b)} Intensities are normalized such that $\sum I_\gamma E_\gamma = 100$ Q. Errors are statistical; the (systematic) calibration error is estimated as 10 %.

^{c)} The capture state is denoted by C.

^{d)} No intensities are listed for these low-energy lines because the efficiency calibration was badly known below $E_\gamma \approx 200$ keV.

^{e)} These γ -rays coincide with known Ge(*n*, γ) lines; the intensities were corrected for the Ge contribution.

states there are eight ($E_x = 2836, 2988, 3123, 3792, 3936, 4137, 4379$ and 5179 keV) showing in-out intensity differences of between 0.5 % and 1.4 % of the capture-state decay. For these levels apparently significant fractions of the feeding or decay intensity are still missing.

In table 3 the bound-state branching ratios are given as derived from the γ -ray intensities in table 1. For the 367 and 706 keV levels these can be compared to the more accurate results (in excellent mutual agreement) from $^{57}\text{Mn}(\beta^-\gamma)$, $^{57}\text{Co}(\text{EC}\gamma)$ and Coulomb excitation, as compiled in ref. ¹⁾. In addition, the branchings of the 1007, 1627 and 1725 keV levels have been measured from the $^{57}\text{Mn}(\beta^-\gamma)$ decay ¹⁾. For the levels below 1.5 MeV the agreement with these previous data is excellent,

TABLE 2

Excitation energies, intensity balance and primary γ -ray branchings for ^{57}Fe levels observed with the $^{56}\text{Fe}(n, \gamma)^{57}\text{Fe}$ reaction

E_x (keV)		Intensity ^{b)}		Primary γ -ray branching ratio (%)
present work ^{a)}	ref. ¹⁾	in	out	
0	0	91(4)		26(3)
14.39(2)	14.4127(4)	55(4)		31(3)
136.48(2)	136.477(2)	2.49(11)		
366.75(2)	366.74(2)	13.9(7)	12.0(5)	6.3(7)
706.39(3)	706.41(2)	4.85(10)	5.61(19)	
1007.26(17)	1007.14(5)	0.48(4)	0.21(2)	
1197.4(5)	1197.8(2)	0.14(3)		
1265.06(5)	1265.1(4)	1.97(14)	2.02(8)	1.16(14)
1357.2(2)	1356.8(3)	0.37(4)		
1627.24(7)	1627.30(7)	11.3(8)	8.85(18)	10.4(9)
1725.39(7)	1725.27(10)	10.7(7)	9.2(3)	10.0(8)
1976.7(2)	1975	0.16(2)	0.08(2)	
2113.0(2)	2117	0.32(5)	0.19(2)	
2206.80(19)	2207	0.60(5)	0.48(7)	
2217.8(2)	(2219(5))	0.23(3)	0.29(5)	
2330.11(18)	2335	0.46(5)	0.05(2)	0.10(4)
2455.1(7)	2454	0.28(2)		
2505.3(2)	2506	0.11(2)	0.20(2)	
2564.2(3)	2565	0.16(2)	0.11(2)	
2599.6(8)	(2597(5))	0.45(6)	0.10(2)	0.17(6)
2697.2(2)	2697.2(10)	1.00(10)	0.76(5)	0.88(10)
2758.33(18)	2763	0.54(2)	0.28(2)	
2821.2(3)	2818	0.08(3)	0.23(2)	0.07(3)
2835.89(14)	2835.0(10)	2.09(11)	1.06(5)	1.93(15)
2855.2(4)	(2855(5))	0.15(5)		
2904.2(3)	2902.3(14)	0.07(2)	0.25(4)	
2921.8(3)	(2920(5))	0.38(3)	0.12(4)	0.30(3)
2971.0(2)	(2974(5))	0.47(2)	0.07(2)	0.41(4)
2987.58(19)	2985	0.09(3)	0.63(5)	0.10(3)
3059.2(4)	3057.6(14)	0.04(1)	0.07(2)	
3099.2(3)	3104	0.10(3)	0.38(3)	
3122.8(3)	(3127(5))	0.02(1)	0.57(19)	
3182.9(2)	3183.2(14)	0.57(5)	0.47(14)	0.54(6)
3205.6(6)	(3207(5))	0.03(1)	0.03(1)	
3240.07(16)	3240.4(10)	1.70(8)	1.21(6)	1.72(12)
3301.89(19)	3302	0.21(1)	0.28(4)	
3322.52(19)	3320.9(14)	0.26(4)	0.66(5)	0.13(4)
3336.8(3)	(3333)	0.13(3)	0.18(2)	
3339.8(7)	3345	0.02(1)	0.28(2)	
3371.3(2)	3369.7(14)	0.28(5)	0.44(3)	0.26(6)
3427.63(13)	3428.6(6)	3.77(19)	3.43(10)	4.0(3)
3535.9(3)	(3535(5))		0.25(2)	
3561.4(2)	3560	0.19(10)	0.29(2)	
3608.7(3)	(3608(5))	0.14(2)	0.08(2)	
3791.57(18)	3790.7(14)	0.19(2)	1.21(8)	0.20(2)
3862.4(3)	3861		0.15(2)	

TABLE 2 (continued)

E_x (keV)		Intensity ^{b)}		Primary γ -ray branching ratio (%)
present work ^{a)}	ref. ¹⁾	in	out	
3936.0(7)	3937		1.34(8)	
3981.7(3)	3979.8(14)	0.49(2)	0.35(5)	0.13(2)
4042.7(3)	4039		0.16(2)	
4136.8(2)	(4138.3(14))	0.05(3)	0.78(11)	0.05(4)
4143.5(5)	4141	0.18(5)	0.10(3)	0.19(5)
4209.6(2)	4208.2(14)	1.63(11)	1.26(7)	1.70(14)
4378.8(2)	4377.8(14)	1.29(5)	0.30(3)	0.35(9)
4459.6(2)	(4459.4(14))	0.68(3)	0.92(6)	0.71(5)
4572.1(5)	4571	0.11(5)	0.15(2)	0.11(6)
4597.5(4)	4594	0.04(1)	0.05(2)	0.04(1)
4691.9(2)	4690.0(14)	0.36(3)	0.62(5)	0.38(3)
5140.2(3)	5139	0.04(1)	0.29(2)	0.04(1)
5178.9(3)	5172	0.08(2)	0.59(6)	0.08(2)
5221.5(4)	5219	0.06(2)	0.30(4)	0.06(3)
5238.4(5)	5234	0.10(2)	0.05(2)	0.11(2)
7646.0(2) ^{c)}			96(5)	

^{a)} From least-squares analysis with E_γ from table 1 (corrected for recoil) as input.

^{b)} Normalization based on $\sum I_\gamma E_\gamma = 100$ Q.

^{c)} Capture state.

but for the decay of the 1627 and 1725 keV levels several new weak branches are observed. The decay of the other 49 states in table 3 is essentially new. Some have been seen in previous (n, γ) work, but a significant comparison with these incomplete data is virtually impossible.

Table 3 also lists the $I_n(d, p)$ values from ref. ¹⁴⁾ and the J^π assignments obtained from (d, p) and other previous work ¹⁾. A comparison of tables 2 and 3 shows that 94 % of the decay of the capture state (with $J^\pi = \frac{1}{2}^+$), including all transitions with intensities exceeding 2 %, proceeds by means of E1 transitions to known p-states ($J^\pi = \frac{1}{2}^-$ or $\frac{3}{2}^-$). Primary transitions of M1 or E2 character to known s- or d-states are quite weak (≤ 0.2 %), except for the relatively strong M1 feeding (1.7 %) of the 3240 keV $\frac{1}{2}^+$ level. No primary transitions are observed to states with $J^\pi = \frac{5}{2}^-$ or $J \geq \frac{7}{2}$.

Remarkably strong (1.9 %) is also the primary to the 2836 keV level for which previous (n, γ) work ¹⁵⁾ had restricted the J^π value to ($\frac{3}{2}, \frac{5}{2}^+$). The fact that this level is weakly (0.7 %) excited ¹⁶⁾ at the $J^\pi = \frac{1}{2}^-$, $E_n = 1.17$ keV (n, γ) resonance with $\Gamma_\gamma = 0.6 \pm 0.1$ eV eliminates the $\frac{5}{2}^+$ possibility. The M2 character of the primary then would lead to a strength of 7 W.u. which exceeds the recommended upper limit ¹⁸⁾ of 3 W.u. The parity of the 2836 keV level is probably odd because even parity would lead to M2 character for the 3 % 2836 \rightarrow 1007 keV decay branch. Apparently, a lifetime measurement is needed for an unambiguous decision on this point. That the knowledge of the lifetime could remove J^π ambiguities also holds

TABLE
Gamma-ray branching ratios (in %) and

E_{xi}	$l_n(\text{d, p})^a)$	$J_i^{\pi b)}$	$\frac{E_{\text{xf}}}{J_i^{\pi c)}$	0 $\frac{1}{2}^-$	14 $\frac{3}{2}^-$	136 $\frac{5}{2}^-$	367 $\frac{7}{2}^-$
367	1	$\frac{3}{2}^-$		13.9(8)	78.8(10)	7.3(5)	
706	3	$\frac{5}{2}^-$		4.8(5)	83.7(8)	9.2(6)	2.3(3)
1007		$\frac{7}{2}^-$			26(6)	74(6)	
1265	1	$\frac{1}{2}^-$			6.1(11)		93.9(11)
1627	1	$\frac{3}{2}^-$		2.35(15)	60.8(9)		28.3(8)
1725	1	$\frac{3}{2}^-$		68.1(13)	2.7(6)		9.9(5)
1977	1	$(\frac{1}{2}, \frac{3}{2})^-$		53(15)			
2113	3	$\frac{5}{2}^-$		81(5)			
2207	3	$\frac{5}{2}^-$		44(7)	52(7)		
2218					44(9)	34(7)	22(5)
2330	1	$(\frac{1}{2}, \frac{3}{2})^-$					
2505	2	$\frac{5}{2}^+$			13(6)		87(6)
2564	1	$\frac{3}{2}^-$		35(7)			
2600				30(9)		70(9)	
2697	1	$\frac{1}{2}^-$		39(3)	57(3)		
2758							78(4)
2821							
2836		$\frac{3}{2}^e)$		24(2)	9.4(14)		
2904	1	$(\frac{1}{2}, \frac{3}{2})^-$					31(9)
2922							
2971							100
2988							7(3)
3059	0	$\frac{1}{2}^+$					100
3099	2	$(\frac{3}{2}, \frac{5}{2})^+$					
3123							100
3183	1	$(\frac{1}{2}, \frac{3}{2})^-$			30(11)		18(6)
3206					100 \rightarrow 2218		
3240	0	$\frac{1}{2}^+$		29(2)	25(4)		30(2)
3302							18(5)
3323	1	$(\frac{1}{2}, \frac{3}{2})^-$					
3337							100
3340	4	$(\frac{7}{2}, \frac{9}{2})^+$			100 \rightarrow 2455		
3371	1	$\frac{3}{2}^-$			77(3)		
3428	1	$\frac{3}{2}^-$			47(2)	9(2)	4.5(5)
3536							
3561	4	$(\frac{7}{2}, \frac{9}{2})^+$					
3609							
3792	2	$\frac{3}{2}^+ d)$			6(3)		
3862							
3936	3	$(\frac{5}{2}, \frac{7}{2})^-$			100		
3982	1	$\frac{3}{2}^-$		28(6) and 39(6) \rightarrow	2600, 29(9) \rightarrow	2697, 4(3) \rightarrow	2821
4043	3	$(\frac{5}{2}, \frac{7}{2})^-$					
4137 $f)$	2	$\frac{5}{2}^+$					
4144 $f)$							
4210	1	$\frac{3}{2}^-(\frac{1}{2}^-)$		5.5(17)	10(2)	16.6(16)	22.9(19)

3

 J^π values of ^{57}Fe bound states (E_γ in keV)

706 $\frac{5}{2}^-$	1007 $\frac{7}{2}^-$	1265 $\frac{1}{2}^-$	1627 $\frac{3}{2}^-$	1725 $\frac{3}{2}^-$	2113 $\frac{5}{2}^-$	2207 $\frac{5}{2}^-$
8.6(5)						
18.9(9)		0.34(11)		47(15)		
		19(5)				
		4(2)				
			100			
				65(7)		
4(2)		22(4)				
	30(7)					and 70(7) \rightarrow 2218
63(2)	2.5(13)				0.8(6)	
69(9)						
100						
		53(3)				and 40(3) \rightarrow 2330
	100					
			10(3)		9(6)	and 17(5) \rightarrow 1357, 16(4) \rightarrow 2971
and 8.2(10) \rightarrow 1977, 4.2(8) \rightarrow 2218, 3.3(7) \rightarrow 2505		30(6)				and 52(7) \rightarrow 1197 and 44(3) \rightarrow 1357, 9.4(19) \rightarrow 1977, 33(2) \rightarrow 2758
			16(2)			and 7(2) \rightarrow 2330
39.9(14)			100			
				28(4)		and 72(4) \rightarrow 2758
	100					
	25(4)	16(2)	40(3)		5.7(9)	and 6.9(10) \rightarrow 2330
					100	
		100				
					7(3)	and 12(3) \rightarrow 2836,
		11(5) \rightarrow 2855, 13(3) \rightarrow 2922, 5.6(14) \rightarrow 3059, 27(4) \rightarrow 3302, 24(10) \rightarrow 3561				
		100				
	6.3(1)	7.2(12)		4(2)		and 2.6(12) \rightarrow 2505,
			5.6(12) \rightarrow 2904, 4.2(8) \rightarrow 3099, 3.8(7) \rightarrow 3183, 10.9(17) \rightarrow 3609			

TABLE 3

E_{xi}	$I_n(d, p)^a)$	$J_i^{\pi b)}$	$E_{xf}:$ $J_f^{\pi c)}$	0 $\frac{1}{2}^-$	14 $\frac{3}{2}^-$	136 $\frac{5}{2}^-$	367 $\frac{3}{2}^-$
4379	1	$\frac{3}{2}^- e)$	53(6)				
4460							
4572	0	$\frac{1}{2}^+$	100 \rightarrow 2600				
4598	2	$\frac{5}{2}^+$	100 \rightarrow 2564				
4692						15(4)	
5140	1	$\frac{1}{2}^-$					
5179	0	$\frac{1}{2}^+$				30(6) and 10(3) \rightarrow 2697,	
5222						33(9)	
5238							

a) From refs. ^{2, 14)}; for the 5140 keV level, see ref. ¹⁷⁾.

b) From refs. ^{2, 15)} if not indicated differently. The levels at 1197 ($\frac{3}{2}^-$), 1357 ($\frac{7}{2}^-$), 2455 ($\frac{7}{2}^+$ or $\frac{5}{2}^+$) and 2855

c) See text.

d) In ref. ¹⁴⁾ $I_n(d, p) = 2$ or 4 is reported; the latter possibility is excluded by the primary (n, γ) feeding.

e) In ref. ¹⁴⁾ $I_n(d, p) = 1$ or 3 is reported; the latter possibility is excluded by the primary (n, γ) feeding.

f) These states are not resolved in the (d, p) work of refs. ^{14, 17)}.

for several higher levels, for instance for those at $E_x = 3099, 3183, 3323, 3561$ and 3936 keV. A good reaction to obtain the missing lifetimes would be $^{54}\text{Cr}(\alpha, n\gamma)^{57}\text{Fe}$.

The reaction Q -value $Q = 7646.0 \pm 0.2$ keV resulting from the present work is compared in table 4 to several previous determinations. For a discussion, see sect. 3.2.

4.2. ^{59}Fe

The 138 γ -rays observed in the $^{58}\text{Fe}(n, \gamma)^{59}\text{Fe}$ reaction are listed in table 5. Of these 68 could be placed in the ^{59}Fe level scheme. The unplaced lines are all weak; the three strongest ($E_\gamma = 2909, 3108$ and 3114 keV) have intensities between 0.5 % and 1.0 %. The energies of the 13 strong lines seen in previous (n, γ) work ⁷⁾ agree within their (large) errors, but some of the intensities are badly off.

The excitation energies of the 28 bound states excited in $^{58}\text{Fe}(n, \gamma)$ are given in table 6. As compared to previous work listed in column two, with which the present work generally is in good agreement, the accuracy has been improved drastically. The existence of the previously dubious levels at 613 and 643 keV could be confirmed. On the whole, the intensity balance is satisfactory although the in-out differences observed for some levels (e.g. those at $E_x = 1162$ and 1211 keV) again point to missing feeding or decay branches.

The present branchings (table 7) for the 287, 571, 726 and 1162 keV levels are in

(continued)

706 $\frac{5}{2}^-$	1007 $\frac{7}{2}^-$	1265 $\frac{1}{2}^-$	1627 $\frac{3}{2}^-$	1725 $\frac{3}{2}^-$	2113 $\frac{5}{2}^-$	2207 $\frac{5}{2}^-$
			17(5)			and 6(3) \rightarrow 3123, 10(3) \rightarrow 3371, 14(4) \rightarrow 4043 and 12.1(18) \rightarrow 2758, 5(2) \rightarrow 3099, 2.1(10) \rightarrow 3340
		58(4)	16(2)	7(3)		
					12(3)	and 6.2(12) \rightarrow 2505, 9.8(19) \rightarrow 2836, 10(2) \rightarrow 2855, 5(2) \rightarrow 3206, 22(3) \rightarrow 3323, 21(4) \rightarrow 3337 40(4)
						and 40(4) \rightarrow 2564, 20(5) \rightarrow 3240
60(6) \rightarrow 3982						
					39(6)	and 28(6) \rightarrow 2836
		100				

keV are weakly excited from higher bound states but the decay is not observed.

whereas $J^\pi = \frac{5}{2}^+$ is excluded in ref. ¹⁵).

whereas $J^\pi = \frac{1}{2}^-$ is excluded in ref. ¹⁵).

agreement with (but more accurate than) those found from the $^{59}\text{Mn}(\beta^-\gamma)$ decay ²⁰). The decay of the 1750, 1919, 1962 and 2447 keV levels turns out to be substantially more fragmented than as found from neutron resonance capture ¹⁶) in which only the strongest branch had been observed. For all other levels the present decay is new.

The J^π value of the 571 keV level had been determined by McLean *et al.* ¹⁹) as $J^\pi = \frac{3}{2}^-$ from (d, p) and (t, p) angular distributions. This was later put in doubt by

TABLE 4
Comparison of Q -values from recent experiments

Q (keV)	Ref.	Reaction	Internal calibration	Absolute calibration
7645.57(35)	³²)	mass spectroscopy		
7646.29(17)	³³)	(n, γ)	6.13 MeV ²⁹) γ -ray from $^{16}\text{O}^*$	^{a)}
7646.0 (2)	^{b)}	(n, γ)	various background lines	$Q(^{15}\text{N})$ ¹¹⁾
7646.02(15)	^{c)}	(n, γ)	$^{14}\text{N}(n, \gamma)$ ³⁴⁾	$Q(^{15}\text{N})$ ¹¹⁾
7645.61(9) ^{d)} }	present work	(n, γ)	$^{35}\text{Cl}(n, \gamma)$ ¹⁰⁾	$Q(^{36}\text{Cl})$ ¹⁰⁾ ^{c)}
7646.04(9) ^{d)} }		(n, γ)	$^{35}\text{Cl}(n, \gamma)$ ⁶⁾	$Q(^{36}\text{Cl})$ ⁶⁾ ^{c)}

^{a)} Absolute calibration of $E_\gamma = 6.13$ MeV ³⁵) is based on $Q(^2\text{H}, ^{13}\text{C}, ^{15}\text{N})$ from ref. ¹¹⁾.

^{b)} Unpublished mean value from refs. ^{10, 12, 13}).

^{c)} In both $^{35}\text{Cl}(n, \gamma)$ measurements ^{6, 10}) the absolute calibration is related to $Q(^{15}\text{N})$ of ref. ¹¹⁾.

^{d)} Only the statistical error is given.

TABLE 5
Gamma-rays from the $^{58}\text{Fe}(n, \gamma)^{59}\text{Fe}$ reaction

$E_\gamma^a)$ (keV)	$I_\gamma^b)$	$E_{x_i} \rightarrow E_{x_f}^c)$ (keV)	$E_\gamma^a)$ (keV)	$I_\gamma^b)$	$E_{x_i} \rightarrow E_{x_f}^c)$ (keV)
280.4(3)	0.38(12)		1719.9(7)	0.72(14)	2447 \rightarrow 726
287.03(2)	59(3)	287 \rightarrow 0	1722.1(4)	0.73(14)	
374.7(4)	0.08(3)		1730.3(8)	0.11(4)	2810 \rightarrow 1078
379.1(4)	0.05(2)		1749.5(3)	0.08(1)	1750 \rightarrow 0
439.43(4)	0.75(4)	726 \rightarrow 287	1904.3(6)	0.07(2)	
465.0(2)	0.23(4)	1078 \rightarrow 613	1918.71(8)	5.69(17)	1919 \rightarrow 0
537.4(7)	0.04(2)	1750 \rightarrow 1211	1956.8(5)	0.15(4)	2570 \rightarrow 613
552.5(5)	0.08(3)		1961.92(18)	0.84(18)	1962 \rightarrow 0
570.81(5)	4.9(3)	571 \rightarrow 0	2084.0(3)	0.19(2)	2810 \rightarrow 726
591.20(3)	3.26(13)	1162 \rightarrow 571	2091.0(3)	0.40(12)	
605.38(17)	0.42(4)		2103.0(3)	0.23(3)	
610.7(2)	0.35(5)	3104 \rightarrow 2494	2138.20(14)	0.37(2)	
613.1(3)	0.20(5)	613 \rightarrow 0	2160.20(6)	2.31(7)	2447 \rightarrow 287
627.3(3)	0.10(2)	3384 \rightarrow 2757	2240.9(3)	0.14(2)	
642.9(3)	0.09(2)	643 \rightarrow 0	2279.3(8)	0.05(2)	2278 \rightarrow 0
670.6(4)	0.07(2)		2322.4(6)	0.28(5)	2321 \rightarrow 0
688.6(5)	0.10(3)	1162 \rightarrow 473	2339.7(3)	0.13(1)	
697.19(16)	0.42(5)	2447 \rightarrow 1750	2361.62(14)	0.32(4)	
699.7(2)	0.36(4)		2428.6(10)	0.06(2)	3160 \rightarrow 726
710.9(4)	0.14(4)		2447.8(2)	0.25(2)	2447 \rightarrow 0
727.4(3)	20.2(8)	726 \rightarrow 0	2494.3(8)	0.05(2)	2494 \rightarrow 0
756.92(12)	0.25(3)	1919 \rightarrow 1162	2505.1(7)	0.08(2)	3072 \rightarrow 571
767.0(6)	0.06(2)		2533.2(3)	0.24(2)	3104 \rightarrow 571
776.9(8)	0.05(2)		2578.4(7)	0.10(2)	
826.9(4)	0.07(2)	3104 \rightarrow 2278	2635.4(2)	0.22(2)	
841.24(12)	0.77(6)	1919 \rightarrow 1078	2751.6(2)	0.33(8)	
875.12(5)	0.95(1)	1162 \rightarrow 287	2872.57(15)	0.30(9)	3160 \rightarrow 287
968.9(9)	0.04(2)		2896.4(5)	0.08(2)	
1048.8(5)	0.10(3)		2908.6(2)	0.62(2)	
1059.1(10)	0.05(3)		2916.2(7)	0.06(1)	
1062.1(5)	0.10(3)	2810 \rightarrow 1750	2948.2(3)	0.30(2)	
1136.9(3)	0.16(3)	2348 \rightarrow 1211	2966.6(3)	0.18(2)	
1162.17(8)	0.48(4)	1162 \rightarrow 0	3057.1(7)	0.05(2)	
1192.50(5)	0.73(4)	1919 \rightarrow 726	3070.4(4)	0.10(3)	3072 \rightarrow 0
1211.24(11)	1.95(12)	1211 \rightarrow 0	3081.4(3)	0.16(3)	
1235.54(4)	2.36(9)	1962 \rightarrow 726	3097.9(9)	0.07(2)	3384 \rightarrow 287
1273.6(3)	0.21(4)		3108.4(5)	0.57(5)	
1323.3(2)	0.08(3)		3114.0(2)	1.0(3)	
1348.4(3)	0.23(8)	1962 \rightarrow 613	3129.2(7)	0.06(2)	
1376.2(9)	0.06(3)		3196.41(10)	0.10(5)	C \rightarrow 3384
1468.3(4)	0.11(3)		3200.3(8)	0.08(3)	
1477.3(4)	0.11(3)		3239.5(3)	1.00(5)	3240 \rightarrow 0
1544.8(9)	0.08(4)	2757 \rightarrow 1211	3337.1(10)	0.04(3)	
1548.8(8)	0.07(3)	2162 \rightarrow 613	3340.8(3)	1.06(5)	C \rightarrow 3240
1551.7(10)	0.06(3)	2278 \rightarrow 726	3422.6(8)	0.06(2)	C \rightarrow 3160
1569.88(8)	0.70(4)	1570 \rightarrow 0	3477.8(13)	0.06(2)	C \rightarrow 3104
1598.79(16)	0.59(4)	2810 \rightarrow 1211	3502.2(3)	0.43(7)	
1647.6(3)	0.36(6)		3513(2)	0.04(2)	C \rightarrow 3072

TABLE 5 (continued)

E_γ ^{a)} (keV)	I_γ ^{b)}	$E_{x_i} \rightarrow E_{x_f}$ ^{c)} (keV)	E_γ ^{a)} (keV)	I_γ ^{b)}	$E_{x_i} \rightarrow E_{x_f}$ ^{c)} (keV)
3523.4(5)	0.12(5)		4757.8(2)	0.42(6)	
3532.1(3)	0.22(2)		4763.8(8)	0.17(3)	
3590.0(5)	0.33(3)		4923.2(4)	0.21(4)	
3664.4(7)	0.19(7)		5009.2(6)	0.37(11)	C \rightarrow 1570
3757.3(9)	0.08(2)		5136(2)	0.07(4)	
3770.5(4)	0.33(4)	C \rightarrow 2810	5204.3(13)	0.11(4)	
3824.0(3)	0.13(2)	C \rightarrow 2757	5369.1(3)	0.33(10)	C \rightarrow 1211
3862(2)	0.06(3)		5375.4(11)	0.26(7)	
4011.5(4)	0.71(11)	C \rightarrow 2570	5383.3(7)	0.19(8)	
4035.7(7)	0.07(2)		5419.5(2)	7.1(11)	C \rightarrow 1162
4072.5(3)	0.18(7)		5565.3(5)	0.40(5)	
4114.2(10)	0.12(3)		5573.9(6)	0.36(6)	
4126.0(8)	0.13(3)		5611.7(10)	0.28(6)	
4133.4(2)	3.58(18)	C \rightarrow 2447	5672.2(7)	0.17(3)	
4164.3(5)	0.31(4)		5854.25(9)	14.9(15)	C \rightarrow 726
4260.0(2)	0.39(3)	C \rightarrow 2321	6012.7(7)	0.54(10)	C \rightarrow 571
4418.7(5)	0.49(5)	C \rightarrow 2162	6097.0(5)	0.19(4)	
4508.0(4)	0.45(7)		6104.4(8)	0.23(7)	
4618.86(12)	3.4(6)	C \rightarrow 1962	6228.4(13)	0.20(9)	
4628.7(8)	0.33(3)		6293.63(10)	47(5)	C \rightarrow 287
4661.81(16)	8.2(10)	C \rightarrow 1919	6580.89(11)	3.4(4)	C \rightarrow 0
4729.5(14)	0.07(3)				

^{a)} Errors are statistical; to account for the uncertainty in the energy calibration, a systematic error of 25 ppm should be added quadratically.

^{b)} Intensities are normalized such that $\sum I_\gamma E_\gamma = 100$ Q. Errors are statistical; the (systematic) calibration error is estimated as 10 %.

^{c)} The capture state is denoted by C.

Warburton *et al.* ²¹⁾ who excited the level in heavy-ion fusion-evaporation reactions. Their γ -ray angular distribution measurements favoured $J^\pi = \frac{5}{2}^-$. The latter possibility is excluded by the present observation of a primary to the 571 keV level which then would have M2 character. The “strong argument” handled by the compilers of Nuclear Data Sheets states that primaries in thermal neutron capture can only have E1, M1, or E2 character.

It must be noted that the 571 keV level is also excited in p-wave neutron capture via the 230 and 359 eV resonances as reported in ref. ¹⁶⁾. Epithermal neutrons are present in the neutron beam used, because the 846 keV γ -transition ascribed to the $^{56}\text{Fe}(n, n' \gamma)$ reaction has been observed. With the help of the known neutron energy spectrum of the high-flux reactor, however, it can be shown that in the present work p-wave neutron capture via the above-mentioned resonances is negligible so that the 571 keV level is excited purely via the s-wave channel at thermal energy.

The 2570, 3072, 3104, 3160 and 3384 keV levels had obtained $L = 2$ and thus $J^\pi = (\frac{3}{2}, \frac{5}{2})^-$ from the (t, p) work ¹⁹⁾. The same argument used above (primary feeding) excludes $J^\pi = \frac{5}{2}^-$ and thus determines $J^\pi = \frac{3}{2}^-$ for these levels.

TABLE 6

Excitation energies, intensity balance and primary γ -ray branchings for ^{59}Fe levels observed with the $^{58}\text{Fe}(n, \gamma)^{59}\text{Fe}$ reaction

E_x (keV)		Intensity ^{c)}		Primary γ -ray branching ratio (%)
present work ^{a)}	previous work ^{b)}	in	out	
0	0	100(3)		3.7(5)
287.00(6)	287.0(3)	52(5)	59(3)	51(3)
473.4(5)	472.70(10)	0.10(3)		
570.84(6)	570.84(13)	4.11(17)	4.9(3)	0.58(12)
613.03(13)	(614(8))	0.68(10)	0.20(5)	
642.9(3)	(639(8))		0.09(2)	
726.44(6)	726.3(3)	19.0(15)	21.0(8)	16(2)
1077.79(14)	1081(16)	0.88(7)	0.23(4)	
1162.07(5)	1161.8(4)	7.4(11)	4.78(14)	7.7(12)
1211.39(13)	1210.6(10)	1.19(12)	1.95(12)	0.35(11)
1569.94(13)	1572(10)	0.37(11)	0.70(4)	0.40(12)
1749.8(2)	1747.3(15)	0.52(6)	0.11(2)	
1918.92(10)	1917.3(15)	8.2(10)	7.45(19)	8.8(11)
1961.98(11)	1962.0(15)	3.4(6)	3.43(14)	3.6(7)
2162.1(5)	2158(10)	0.49(5)	0.07(3)	0.53(7)
2278.0(4)	2273(10)	0.07(2)	0.11(4)	
2321.0(2)	2321(10)	0.39(3)	0.28(5)	0.42(4)
2348.3(3)	2345(10)		0.16(3)	
2447.25(13)	2446.0(15)	3.58(18)	3.69(17)	3.9(3)
2493.8(4)	2488(10)	0.35(5)	0.05(2)	
2569.6(4)	2565	0.71(11)	0.15(4)	0.77(12)
2756.9(3)	2759	0.23(3)	0.08(4)	0.14(2)
2810.4(2)	2812(10)	0.33(4)	0.98(7)	0.35(5)
3071.5(4)	3071	0.04(2)	0.18(4)	0.05(2)
3104.4(3)	3103	0.06(2)	0.66(6)	0.06(3)
3160.0(2)	3160	0.06(2)	0.36(9)	0.06(2)
3239.8(2)	3235(10)	1.06(5)	1.00(5)	1.14(9)
3384.3(2)	3388(10)	0.10(5)	0.17(3)	0.10(5)
6581.0(2) ^{d)}			92(6)	

^{a)} From least-squares analysis with E_γ from table 5 (corrected for recoil) as input.

^{b)} From refs. ^{2, 16, 20, 21}.

^{c)} Normalized such that $\sum I_\gamma E_\gamma = 100 Q$.

^{d)} Capture state.

The $^{58}\text{Fe}(n, \gamma)^{59}\text{Fe}$ primary decay also mainly proceeds (84 %) via E1 transitions to p-states. In addition, there are strong primaries to the levels at 1919 keV (8.2 %) and 2447 keV (3.9 %). The latter level is not excited in the (d, p) reaction, whereas the $l(d, p)$ value of the former could not be determined ¹⁹). Notable is also the relatively strong (1.1 %) M1 primary to the 3240 keV level with $J^\pi = (\frac{1}{2}, \frac{3}{2})^+$.

It is improbable that the (n, γ) reaction excites the known $\frac{7}{2}^-$ level at 1023 keV. This level, located by Warburton *et al.* ²¹) at $E_x = 1023.12 \pm 0.13$ keV, shows decay branches to $^{59}\text{Fe}(0)$ and to the 473 and 571 keV levels ²¹). No $\frac{1}{2}^+ \rightarrow \frac{7}{2}^-$ (n, γ) primary

TABLE 7
Gamma-ray branching ratios (in %) and J^π values of ^{59}Fe bound states (E_x in keV)

E_x	$L_n(d, p)^a$	$J^\pi{}^b$	$E_{\text{ref}}:$ $J^\pi:$	0 $\frac{1}{2}^-$	287 $\frac{1}{2}^-$	571 $\frac{3}{2}^-$	613	726 $\frac{3}{2}^-$	1078 $(\frac{1}{2}, \frac{3}{2})^-$	1211 $\frac{1}{2}^-$	1750 $(\frac{3}{2}, \frac{3}{2})^-$
287	1	$\frac{1}{2}^-$	100								
571	1	$\frac{3}{2}^-$	100								
613			100								
643			100								
726	1	$\frac{3}{2}^-$	96.4(2)		3.6(2)						
1078	1	$(\frac{1}{2}, \frac{3}{2})^-$					100				
1162	1	$\frac{3}{2}^-$	10.0(9)		19.9(6)	68.0(11) and 2.1(4) → 473					
1211	1	$\frac{1}{2}^-$	100								
1570	3	$\frac{3}{2}^-$	100								
1750		$(\frac{3}{2}, \frac{3}{2})^-$	68(13)							32(13)	
1919		$(\frac{3}{2}, \frac{3}{2})^+$	76.4(10)					9.8(6)	10.4(8) and 3.4(3) → 1162		
1962	1	$\frac{1}{2}^-$	25(2)				7(2) 100	68(2)			
2162								52(15)			
2278			48(15)								
2321			100								
2348											
2447		$(\frac{3}{2}, \frac{3}{2})^+$	6.7(6)		63(3)			19(3)		100	11.3(14)
2494			100								
2570		$\frac{3}{2}^-$					100				
2757											
2810	1	$\frac{1}{2}^-$									
3072		$\frac{3}{2}^-$									
3104		$\frac{3}{2}^-$	54(11)			46(11)		19(2)	11(4)	100	60(4)
3160		$\frac{3}{2}^-$				36(4) and 10(3) → 2278, 54(4) → 2494					
3240		$(\frac{1}{2}, \frac{3}{2})^+$	100		84(4)			16(4)			
3384		$\frac{3}{2}^-$			41(12) and 59(12) → 2757						

^{a)} From ref. ¹⁹⁾.

^{b)} From refs. ^{2, 15, 19)} and present work (see text); the 473 keV level (of which the decay is not observed) has $J^\pi = \frac{3}{2}^-$.

is expected, nor has it been observed. None of the three decay transitions given in ref. ²¹⁾ are observed either. One might tentatively consider the unplaced 2138 and 2362 keV lines as feeding the level from the 3160 and 3384 keV levels, respectively, whereas the unplaced 379 keV line might deexcite the level to the 643 keV level. Apart from the fact that the decay would be different, there are several additional arguments against such an interpretation, however. The excitation energy found from a least-squares fit would be 1022.2 ± 0.2 keV, differing by 0.9 ± 0.2 keV from that given in ref. ²¹⁾. There would be a considerable intensity imbalance (0.69 % in, against 0.05 % out) for the 1022 keV level, and the intensity balances for the 3160 and 3184 keV levels would also become worse.

The Q -value of the $^{58}\text{Fe}(n, \gamma)^{59}\text{Fe}$ reaction is determined from the present work as 6581.0 ± 0.2 keV, in excellent agreement with (but much more accurate than) the value 6581.0 ± 2.2 keV following from the 1977 atomic mass evaluation ³⁰⁾.

5. A shell-model calculation on $^{57-59}\text{Fe}$

No detailed shell-model calculations have been published on ^{57}Fe and ^{59}Fe . The calculations on ^{57}Fe of Johnstone and Benson ²⁵⁾ and of McGrory ²⁶⁾ did not consider electromagnetic properties. The latter are discussed by Bolotin *et al.* ²⁴⁾ but only for the three lowest states of ^{57}Fe . For ^{59}Fe only excitation energies are discussed by Warburton *et al.* ²¹⁾ and by McGrory ²⁷⁾. In all these calculations the model space was restricted to two $1f_{7/2}$ proton holes and neutrons in the $2p_{3/2}$, $1f_{7/2}$ and $2p_{1/2}$ orbits.

The present shell-model calculation has been performed on the $^{57-59}\text{Fe}$ nuclei in the same model space as used in the calculations mentioned above. The even-mass nucleus ^{58}Fe has been taken into account for a better determination of the interaction parameters from a least-squares fit. Two interactions have been investigated, i.e. a modified Kuo-Brown interaction (KB) and the surface delta interaction (SDI), which both have not yet been applied to these nuclei. The KB and SDI two-body matrix elements are discussed in refs. ^{22, 23)}, respectively.

The strength parameters for the $T = 0$ and $T = 1$ matrix elements, i.e. A_0 and A_1 for SDI as well as C_0 and C_1 for KB together with the single-particle energies are obtained from a least-squares fit of 22 theoretical excitation energies to the corresponding experimental values. The levels in fig. 2 indicated with a dot have been used for this purpose. The resulting parameter values are given in table 8. It follows from fig. 2 that for the low-energy parts of the spectra, where experimental spin assignments are reliable, a nice one-to-one correspondence exists between experimental states and their theoretical counterparts. For the 22 levels used in the fitting procedure the average deviation between theoretical and experimental excitation energies is small, amounting to about 0.17 MeV for both KB and SDI. Thus the two interactions appear to produce equivalent spectra in this model space with no

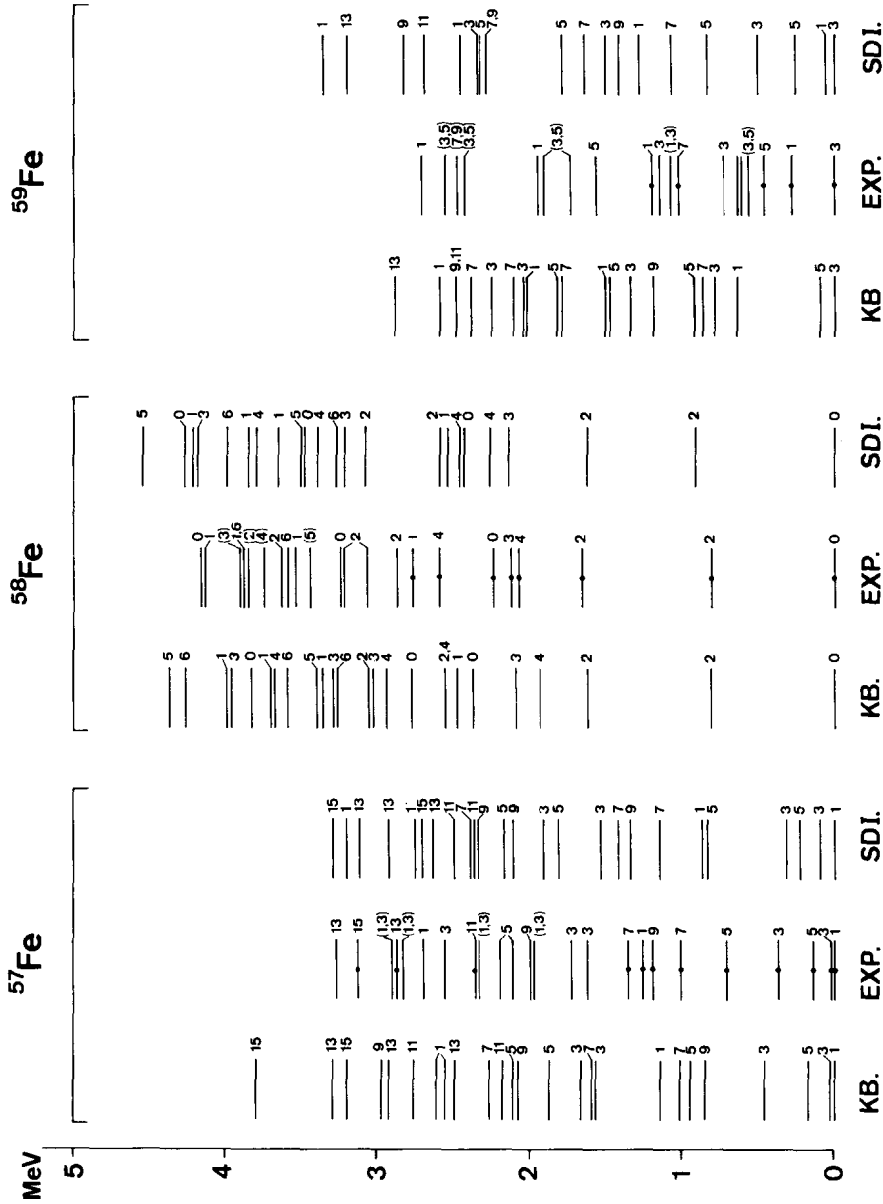


Fig. 2. Comparison of experimental and calculated energy level spectra of $^{57-59}\text{Fe}$. The experimental information (levels with $\pi = +$ in ^{58}Fe and $\pi = -$ in $^{57,59}\text{Fe}$) is extracted from refs. ^{1,2,3,11} and the present work. The levels indicated with a dot are used in the fitting procedure. For the interactions denoted by KB and SDI see text. For the odd- A nuclei, $2J$ rather than J is indicated, for brevity.

TABLE 8

Parameter values (in MeV) used in the shell-model calculations with the SDI and KB interactions

		SDI	KB
Interaction strengths	$T = 0$	$A_0 = 0.93$	$C_0 = 1.21$
	$T = 1$	$A_1 = 0.54$	$C_1 = 1.21$
Relative ^{a)} single-particle energies	$\epsilon_{5/2} - \epsilon_{3/2}$	0.87	3.67
	$\epsilon_{1/2} - \epsilon_{3/2}$	0.80	1.44

^{a)} Defined with respect to the ^{40}Ca core.

clear preference for either. This result does not hold, however, for the electromagnetic properties (see below).

The present wave functions have been used to calculate branching ratios, life-times and moments of many states in ^{57}Fe only. The electromagnetic properties of ^{59}Fe , although investigated experimentally as discussed in this paper, have not been considered since (i) experimental information is limited to the presently determined branching ratios and (ii) the spins of the 146 keV and 643 keV levels are not known. The knowledge of the latter values is crucial for a meaningful comparison between theory and experiment.

It turned out that for ^{57}Fe reasonable agreement with experimental values could be obtained when the values of all M1 single-particle matrix elements were reduced

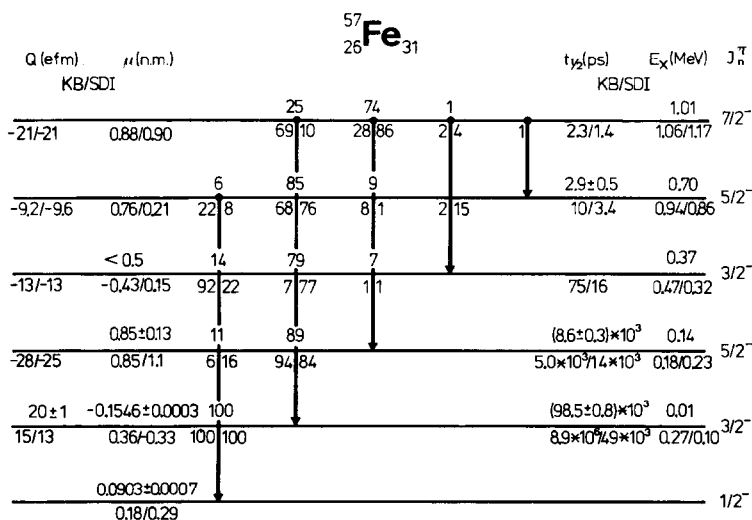


Fig. 3. Comparison of experimental and calculated electromagnetic properties of the lowest six states of ^{57}Fe . The experimental information is from ref. ¹⁾. The experimental data are indicated above the lines, the theoretical data below the lines, with those obtained by means of the KB interaction to the left and those obtained with the SDI interaction to the right of the division sign.

by a factor of two. Furthermore quite large effective charges given by $e_p = 2e$ and $e_n = e$ had to be introduced. The ^{57}Fe results for KB and SDI are compared in fig. 3 with experiment, which includes the present experimental data. It follows from fig. 3 that the SDI values agree reasonably well with the experimental data, whereas KB yields a considerably worse agreement for electromagnetic properties. This is an important result since recent calculations ²²⁾ on $^{54-56}\text{Fe}$ including up to three $f_{7/2}$ holes strongly favour the KB interaction. The conclusion must be that for states described by at most two $f_{7/2}$ holes and several particles in the upper orbits SDI is superior whereas KB is favoured when the $f_{7/2}$ hole structure dominates the wave functions. This conclusion supports that reached in ref. ²⁸⁾ on the same subject. The theoretical transition rates for states above the lowest $J^\pi = \frac{7}{2}^-$ state are in poor agreement with experiment for both interactions and are hence omitted from fig. 3. The model space is apparently too small for a reliable description of the higher-lying states.

It is interesting to compare the calculated properties with those of Bolotin *et al.* ²⁴⁾, which are restricted to the yrast $J^\pi = \frac{1}{2}^-$, $\frac{3}{2}^-$ and $\frac{5}{2}^-$ states. One finds that the present SDI results are somewhat superior despite the state-dependent effective transition operators used in ref. ²⁴⁾.

The need for a strong reduction of the M1 matrix elements as well as for a large effective charge must be related to the restrictions on the model space. From recent calculations ²²⁾ on $^{54-56}\text{Fe}$ it follows that $(f_{7/2})^{-3}$ admixtures do not decrease with increasing mass from ^{54}Fe to ^{56}Fe . An $(f_{7/2})^{-3}$ admixture of about 40 % is obtained ²²⁾ for low-lying states in ^{56}Fe . Hence, there is no reason to assume that these admixtures in ^{57}Fe can be ignored. From the present results we can conclude that effects of these three-hole admixtures cannot easily be absorbed in effective transition operators. However, exact three-hole calculations on ^{57}Fe would require the construction and diagonalisation of very large matrices, which is beyond the scope of this paper.

6. Conclusions

The present work has provided accurate excitation energies and γ -ray branching ratios of a great many low-spin levels in ^{57}Fe and ^{59}Fe . It has led to spin restrictions of levels in both nuclei and to the unambiguous J^π determination of five levels in ^{59}Fe . In addition, the Q -values of the $^{56,58}\text{Fe}(n, \gamma)$ reactions have been determined.

The primary branchings to final p-states yield information on the capture mechanism at thermal energy. For direct or valence capture one would expect the primary intensities (divided by E_γ^k , with $k \approx 1$ or 2) and the spectroscopic factors $(2J+1)S$ found from the (d, p) reaction to be correlated. Excellent correlations, with correlation coefficients very close to unity are found for instance for many nuclei in the mass region $A = 20-65$ [ref. ¹³⁾]. The present data clearly show that

for ^{56}Fe and ^{58}Fe neither direct nor valence capture is predominant. The correlation between the I_γ/E_γ values from the present work and the (d, p) spectroscopic factors from ref. ¹⁴⁾ for ^{56}Fe and from ref. ¹⁹⁾ for ^{58}Fe is terrible. The ratios $(2J+1)SE_\gamma/I_\gamma$ vary by factors of at least 100 and 2000 for ^{56}Fe and ^{58}Fe , respectively.

Shell-model calculations have been performed on the $^{57,58,59}\text{Fe}$ isotopes. Two rather different effective two-body interactions (KB and SDI) have been investigated. In the model space two $f_{7/2}$ proton holes with neutrons in the $p_{3/2}$, $f_{5/2}$ and $p_{1/2}$ orbits are taken into account. The two interactions reproduce the energy spectra equally well but deviate quite strongly for the electromagnetic properties in ^{57}Fe . It turns out that SDI is superior in this model space. Both interactions fail to reproduce the experimentally known branching ratios of the levels above the yrast $J^\pi = \frac{7}{2}^-$ state in ^{57}Fe . This and the need for effective M1 operators and a large effective charge indicates that the model space used in the present and previous theoretical studies is too restricted for a reasonable microscopic description of ^{57}Fe . The available experimental data on electromagnetic properties of ^{59}Fe are still insufficient for a critical evaluation of the theory.

We would like to thank Dr. K. Abrahams and Dr. C. van der Leun for very useful discussions regarding the present results.

This work was performed as part of the research programma of the "Stichting voor Fundamenteel Onderzoek der Materie" (FOM) with financial support from the "Nederlandse Organisatie voor Zuiver-Wetenschappelijk Onderzoek" (ZWO).

References

- 1) R. L. Auble, Nucl. Data Sheets **20** (1977) 327
- 2) H. J. Kim, Nucl. Data Sheets **17** (1976) 485
- 3) G. A. Bartholomew *et al.*, Nucl. Data **A3** (1967) 367
- 4) E. A. Eissa and J. Honzátko, Z. Phys. **243** (1971) 114
- 5) V. J. Orphan, N. C. Rasmussen and T. L. Harper, MIT-Report CA-10248 (1970)
- 6) M. L. Stelts and R. E. Chrien, Nucl. Instr. **155** (1978) 253
- 7) A. P. Bogdanov, V. A. Knat'ko, A. V. Soroka and V. N. Tadéush, Yad. Fiz. **14** (1971) 909; Sov. J. Nucl. Phys. **14** (1972) 509
- 8) R. Gunnink, R. A. Meyer, J. B. Niday and R. P. Anderson, Nucl. Instr. **65** (1968) 26
- 9) C. Meixner, Jülich Report Jül.-1087-Rx (1974)
- 10) A. M. J. Spits and J. Kopecky, Nucl. Phys. **A264** (1976) 63
- 11) L. G. Smith and A. H. Wapstra, Phys. Rev. **C11** (1975) 1392
- 12) A. M. J. Spits, A. M. F. Op den Kamp and H. Gruppelaar, Nucl. Phys. **A145** (1970) 449
- 13) A. M. J. Spits and J. A. Akkermans, Nucl. Phys. **A215** (1973) 260;
J. Kopecky and C. Plug, Netherlands Energy Research Foundation Report RCN-75-004 (1975)
- 14) H. M. Sen Gupta, A. R. Majumder and E. K. Lin, Nucl. Phys. **A160** (1971) 529
- 15) R. Vennink, W. Ratynski and J. Kopecky, Nucl. Phys. **A299** (1978) 429
- 16) J. C. Wells, S. Raman and G. G. Slaughter, Phys. Rev. **C18** (1978) 707
- 17) J. A. Thomson, Nucl. Phys. **A227** (1974) 485
- 18) P. M. Endt, Atomic Data and Nucl. Data Tables **23** (1979) 3
- 19) K. C. McLean, S. M. Dalglish, S. S. Ipson and G. Brown, Nucl. Phys. **A191** (1972) 417
- 20) R. C. Pardo *et al.*, Phys. Rev. **C16** (1977) 370

- 21) E. K. Warburton *et al.*, Phys. Rev. **C16** (1977) 1027
- 22) R. Vennink and P. W. M. Glaudemans, Z. Phys., to be published
- 23) P. J. Brussaard and P. W. M. Glaudemans, Shell-model applications in nuclear spectroscopy (North-Holland, Amsterdam, 1977)
- 24) H. H. Bolotin, A. E. Stuchbery, K. Amos and I. Morrison, Nucl. Phys. **A311** (1978) 75
- 25) I. P. Johnstone and H. G. Benson, Phys. Rev. **C17** (1978) 311
- 26) J. B. McGrory, Phys. Lett. **21** (1966) 64
- 27) J. B. McGrory and S. Raman, Phys. Rev. **C20** (1979) 1830
- 28) A. G. M. van Hees, P. W. M. Glaudemans and B. C. Metsch, Z. Phys. **A293** (1979) 327
- 29) J. Kopecky, K. Abrahams and F. Stecher Rasmussen, Nucl. Phys. **A188** (1972) 535; **A215** (1973) 45
- 30) A. H. Wapstra and K. Bos, Atomic Data and Nucl. Data Tables **19** (1977) 177
- 31) D. C. Kocher and R. L. Auble, Nucl. Data Sheets **19** (1976) 445
- 32) J. W. Barnard *et al.*, Can. J. Phys. **55** (1977) 200
- 33) D. E. Alburger, Nucl. Instr. **136** (1976) 323
- 34) R. C. Greenwood and R. G. Helmer, Nucl. Instr. **121** (1974) 385
- 35) E. B. Shera, Phys. Rev. **C12** (1975) 1003